

**NASA TECHNICAL  
MEMORANDUM**



**NASA TM X-3033**

**NASA TM X-3033**

**CASE FILE  
COPY**

**PARAMETRIC STUDY OF ION HEATING  
IN A BURNOUT DEVICE (HIP-1)**

*by Donald R. Sigman, John J. Reinmann,  
and Milton R. Lauver*

*Lewis Research Center  
Cleveland, Ohio 44135*



1. Report No. NASA TM X-3033	2. Government Accession No.	3. Recipient's Catalog No.	
4. Title and Subtitle PARAMETRIC STUDY OF ION HEATING IN A BURNOUT DEVICE (HIP-1)		5. Report Date APRIL 1974	6. Performing Organization Code
		8. Performing Organization Report No. E-7766	
7. Author(s) Donald R. Sigman, John J. Reinmann, and Milton R. Lauver		10. Work Unit No. 502-10	11. Contract or Grant No.
9. Performing Organization Name and Address Lewis Research Center National Aeronautics and Space Administration Cleveland, Ohio 44135		13. Type of Report and Period Covered Technical Memorandum	
		14. Sponsoring Agency Code	
12. Sponsoring Agency Name and Address National Aeronautics and Space Administration Washington, D. C. 20546		15. Supplementary Notes	
16. Abstract Results of further studies on the Lewis Research Center hot-ion-plasma source (HIP-1) are reported. Changes have been made in both the electrode geometry and materials to produce higher ion temperatures. Ion temperature increased significantly with increased vacuum pumping speed. The best ion temperatures achieved, so far, for H <sup>+</sup> , D <sup>+</sup> , and He <sup>+</sup> plasmas are estimated to be $\geq 0.6$ , $\geq 0.9$ , and $\geq 2.0$ keV, respectively. Electrode pairs produced high ion temperatures whether on the magnetic axis or off it by 5.5 cm. Multiple sources, one on-axis and one off-axis, were run simultaneously from a single power supply by using independent gas feed rates. A momentum analyzer has been added to the charge-exchange neutral particle analyzer to identify particles according to mass, as well as energy. Under any given plasma condition, the higher mass ions have higher average energies but not by as much as the ratio of their respective masses.			
17. Key Words (Suggested by Author(s)) Ion heating Hot-ion plasma		18. Distribution Statement Unclassified - unlimited Category 25  CAT. 25	
19. Security Classif. (of this report) Unclassified	20. Security Classif. (of this page) Unclassified	21. No. of Pages 17	22. Price* \$ 3.00

\* For sale by the National Technical Information Service, Springfield, Virginia 22151

# PARAMETRIC STUDY OF ION HEATING IN A BURNOUT DEVICE (HIP-1)

by Donald R. Sigman, John J. Reinmann, and Milton R. Lauver

Lewis Research Center

## SUMMARY

Results of further studies on the Lewis Research Center hot-ion-plasma source (HIP-1) are reported. Changes have been made in both the electrode geometry and materials to increase plasma ion temperatures and thus optimize performance. Ion temperature increased significantly with increased vacuum pumping speed. The best ion temperatures achieved, so far, for  $H^+$ ,  $D^+$ , and  $He^+$  plasmas are estimated to be  $\geq 0.6$ ,  $\geq 0.9$ , and  $\geq 2.0$  keV, respectively. Electrode pairs produced high ion temperatures whether on the magnetic axis or off it by 5.5 centimeters. Multiple sources, one on-axis and one off-axis, were run simultaneously from a single power supply, by using independent gas feed rates.

A momentum analyzer has been added to the charge-exchange neutral particle analyzer to identify particles according to mass, as well as energy. Under any given plasma condition, the higher mass ions have higher average energies but not by as much as the ratio of their respective masses.

## INTRODUCTION

This report discussed several experiments done on the HIP-1 (hot-ion-plasma) source (ref. 1) at the NASA Lewis Research Center. The purpose of the experiments was to determine how ion heating is affected by various changes in the electrode geometry, positioning, and materials; the system vacuum pumping; and the applied voltages and magnetic fields. Work was done for three gases: hydrogen, deuterium, and helium.

In the HIP-1 facility energy is coupled to the plasma by applying a radially inward direct current electric field near the maximum field region of a magnetic mirror. Under the influence of the radial electric field  $\mathcal{E}$  and the axial magnetic field  $B$ , the ions drift azimuthally with a velocity  $\mathcal{E}/B$ . The energy corresponding to this drift velocity  $\left[ \frac{1}{2} m(\mathcal{E}/B)^2 \right]$  can be several kilovolts. It has been predicted theoretically

(ref. 2) and determined experimentally (ref. 3) that high-frequency (on the order of the ion plasma frequency) electrostatic drift waves also are present in this type of plasma configuration. It is possible that the fields of these waves heat the plasma ions to energies greater than the drift energy.

The principal diagnostic used in these parametric studies was a neutral particle energy analyzer for estimating ion temperature. It was assumed that the plasma density was not appreciably changed from its nominal value ( $\sim 10^{12}/\text{cm}^3$ ) by any of the parametric changes. Therefore, any change which resulted in an increased ion temperature represented an improvement in source performance.

### SYMBOLS

a	distance from anode tip to cathode tip (see fig. 1(b)), cm
B	magnetic field strength, T
$B_0$	magnetic field strength at midplane, T
b	cathode diameter, cm
c	anode-cathode gap (see fig. 1(b)), cm
E	ion energy, keV
$E_p$	ion energy corresponding to maximum in $I(E)$ , keV
$E_{\text{drift}}$	drift energy $\left[ E_{\text{drift}} = 1/2 m (\mathcal{E}/B)^2 \right]$
$\mathcal{E}$	electric field strength
e	electronic charge
$I(E)$	MEM detector current
K	Boltzmann's constant
m	ion mass
R	radius of curvature of magnetic field line
T	ion temperature
$V_a$	applied voltage between anode and cathode
$v_D$	drift velocity ( $v_D = \mathcal{E}/B$ )
$W_{11}$	ion energy component parallel to magnetic field direction
$\eta$	constant in the expression approximating $I(E)$ as $E^\eta e^{-E/kT}$

## DESCRIPTION OF THE EXPERIMENT AND DIAGNOSTICS

A schematic of the overall experimental apparatus is shown in figure 1(a); a more detailed view of the electrode structure is given in figure 1(b). The maximum value of the magnetic field at the midplane  $B_0$  was 1.5 tesla, and the mirror ratio was 1.82. The voltage available to be applied to the electrodes was 20 kilovolts. The gas feed was always through the center of the hollow cathodes. The facility is such that various lengths and diameters of both anodes and cathodes can be tested at a variety of positions within the vacuum vessel. For the data presented herein, the gas flow rate through the cathodes is always adjusted so that the plasma operates in the high resistance ion heating mode discussed in reference 1.

The principal diagnostic tool was the neutral particle analyzer (NPA) shown in figure 2. After emerging from the plasma, the charge-exchanged neutrals are collimated and then reionized in a nitrogen gas stripping cell. The charged particles are then separated according to energy by passing them through the  $90^\circ$  electrostatic deflection plates. If the detector, which was a Bendix model 306 magnetic electron multiplier (MEM), is placed at position 1 (fig. 2), immediately behind the output slit of the deflection plates, the detector current as a function of energy  $I(E)$  can be determined by sweeping the voltage on the plates. A complete sweep takes just a few seconds. These spectra do not distinguish particles according to mass, only energy. If the detector at position 1 is pulled out, the ions of a given energy pass into a bending magnetic field; then the various mass species can be separated. Thus, for a given voltage on the electrostatic deflection plates there exists a magnetic field for which only ions of a given energy and mass can pass through the slit and be detected at position 2. Use of the complete analyzer allows one to determine  $I(E)$  for each mass separately. The MEM output current was fed into a Keithley model 417 picoammeter.

The NPA sampled, from along a chord of plasma, a region approximately 1 centimeter high (vertical) and 2.5 centimeters wide (parallel to the magnetic field). The NPA apparatus was mounted so that the plasma could be scanned vertically by pivoting the beam line about a point located at the test section flange (see fig. 2).

It is extremely difficult to obtain an accurate energy distribution within the plasma from the energy distribution at the detector output  $I(E)$ . The difficulty arises because there is an uncertainty in the energy dependence of those factors that relate the detector current to the plasma ion energy distribution (ref. 1). These factors include the charge-exchange between plasma ions and the neutral background gas, the nitrogen gas stripping cell conversion efficiency, the secondary emission coefficient for the MEM cathode, and also the effects of plasma rotation and large ion gyroradii.

Near the peak in the spectrum,  $I(E)$  would have the general form  $E^\eta e^{-E/kT}$  for a Maxwellian ion energy distribution in the plasma. The value of  $\eta$  was estimated to be

between 3 and 4. The energy at the peak  $E_p$  would be related to the ion temperature of the dominant species by the relation  $kT = E_p/\eta$ . Thus, for much of the data presented herein, one can determine the relative performance of the ion heating scheme by looking at how  $E_p$  changes with various parameters.

## CATHODE-ANODE MATERIALS

Carbon cathodes and anodes were used in the Burnout series at Oak Ridge National Laboratory and initially in the HIP-1 facility. From the nature of some of the NPA data presented in reference 1, it was thought that the high-energy tail of the current distribution function  $I(E)$  was composed primarily of carbon ions; and, as will be shown later, this turned out to be true. It was thought that it would be desirable to go to an all metal (noncarbon) electrode system. The first change was to fabricate and install tungsten cathodes. But no significant reduction in the high energy tail of the current function  $I(E)$  resulted. Thus, it was surmised that the carbon came primarily from either the anodes or the carbon remaining on the walls of the test section. Retaining the tungsten cathodes but replacing the carbon anode with a stainless-steel anode, again, had little immediate effect on the high energy tail. It was concluded that the plasma would still operate in the same ion heating mode with metal electrodes but that the carbon impurity would not disappear immediately. Subsequent running of the facility (for several weeks) did significantly reduce the carbon component, but it never disappeared completely. The carbon and tungsten cathodes were similar in operating temperatures, with the tips being about  $1400^{\circ}$  to  $1500^{\circ}$  C. Any attempt to raise the temperatures above these values always lead to the high-current - low ion temperature mode discussed in reference 1.

The operating pressure (i. e. , gas flow rate) for the ion heating mode was approximately 50 percent higher for tungsten cathodes than for carbon cathodes. One would expect this to result in lower ion temperatures because of an increase in charge-exchange losses with higher pressure. Using  $E_p$  as a measure of relative ion temperature, the temperatures with carbon cathodes are 10 to 15 percent higher than with tungsten cathodes for a given applied voltage  $V_a$  between electrodes. But with the carbon anodes internal arcs would occur in the plasma when  $V_a$  exceeded 12 kilovolts. Tungsten cathodes produced no such internal arcs, and  $V_a$  was limited only by external breakdowns (at about 17 to 18 kV) where the cathode holder enters the vacuum system. As a result of these higher voltages, the best temperatures achieved with tungsten cathodes were about 30 percent higher than those for carbon.

## ELECTRODE DIMENSIONS AND POSITIONING

The HIP-1 data presented in reference 1 was taken using the same anode and cathode lengths and diameters as in the Burnout VI experiments. Also, the positions of the ends of the electrodes relative to the mirror throat were the same. The ends nearer the midplane were exactly at the throat (30 cm from the midplane), and the hot emitting cathode tips were 37.6 centimeters from the midplane (i. e., recessed 7.6 cm into the cylindrical anode). Because it was not known whether this particular geometry was optimum for producing a hot dense plasma, a series of experiments was performed in which a parametric study of ion temperature was made for various electrode dimensions and positions. The relevant dimensions as shown in figure 1(b) are  $a$ , the location of the cathode tip relative to the anode tip ( $a = 7.6$  cm in the original configuration),  $b$ , the diameter of the cathode ( $b = 1.3$  cm originally); and  $c$ , the radial separation of cathodes and anodes ( $c = 1.1$  cm originally).

Figure 3 shows  $E_p$  as a function of the applied voltage  $V_a$  for several values of the cathode tip position  $a$ . The anode length was 15 centimeters, and the gas was helium. It appears that the original position ( $a = 7.6$  cm) is near the optimum. For  $a = 7.6$  and 10.8 centimeters the gas flow rate was the same, but for the other positions, the necessary flow rate to light the discharge was greater. For  $a = 20.3$  centimeters the flow rate was more than double that for  $a = 7.6$  centimeters. It is felt that in this source significant ionization is occurring in three regions: (1) inside the hollow cathode, (2) in the region between the cathode tip and the anode end at the mirror throat, and (3) between the mirrors. The pressure is very high inside the cathodes since the gas feed is through the cathode. Also, the cylindrical anode surrounding the cathode keeps the pressure higher just in front of the tip than it would be if the anode were removed. Whenever the cathode tip is moved too far forward or backward (toward or away from the midplane), the gas trapping effect of the anode is reduced, and it is necessary to increase the gas flow rate to light the discharge. But increased gas flow leads to larger charge-exchange losses and thus to lower ion temperatures.

The effect of changing the cathode-anode gap dimension  $c$  is shown in figure 4 for  $V_a = 10$  kilovolts and the cathode tip at  $a = 7.6$  centimeters. As the gap is reduced (by reducing the anode diameter) and the applied voltage is held constant, the radial electric field should increase. Thus, we see from the data, a corresponding increase in  $E_p$ . For this set of data the required flow rate was changed very little, being slightly more for the larger gaps. The data shown in figure 4 is for an applied voltage  $V_a$  of 10 kilovolts.

The nominal midplane diameter of the plasma for which all data have been presented so far is about 2 centimeters. This is just slightly greater than that of the field lines that intersect the outer edge of the cathode. It is of interest to know if the plasma diameter could be increased by increasing the cathode diameter. Thus 5-centimeter-long

cylindrical tungsten sleeves were machined to fit the end of the cathode tip. The outer diameter of the sleeves was 1.9 centimeters thus increasing the cathode diameter  $b$  by about 50 percent. With the sleeves in place, the shape of the analyzer traces  $I(E)$ , taken while viewing along a chord through the center of the plasma, was essentially unchanged. Profiles of the plasma were then obtained by setting the analyzer to detect various energy particles and then sweeping the line of sight up and down across the plasma column. Figure 5 shows these profiles for both 1.3- and 1.9-centimeter cathodes. It is easy to see that the mean diameter of the plasma did not change in proportion to the external diameter of the cathodes. As a result, it was surmised that the internal diameter of the cathode was controlling the plasma diameter. In the future, hollow cathodes with large internal diameters will be fabricated and tested.

The usual cathodes used in these experiments were hollow for a distance of about 20 centimeters. To test whether this length was optimum, a small tantalum plug with seven small holes was machined and inserted into the hollow cathode. Whenever the plug was recessed more than about 5 centimeters, the performance of the source was unaffected. As the plug was placed nearer the tip, the required gas flow rates increased, and ion temperatures decreased correspondingly. When the plug was flush with the cathode tip the flow rate was approximately double that required in the absence of plugs.

Moving the anode-cathode assemblies 7.6 centimeters farther toward the midplane of the mirrors (cathode tips were recessed 7.6 cm from the anode tips) did not appreciably affect either the gas flow rates or the ion temperatures achieved.

#### EFFECT OF PUMPING RATE

To study the effect of vacuum pumping rate on the ion temperature, an experiment was performed with one, two, three, and then all four the system's diffusion pumps being used. Each time a diffusion pump is switched into the system, it is necessary to increase the gas flow rate through the hollow cathodes to achieve the desirable operating mode. However, the increase is small enough that the pressure (density of cold neutrals) at the midplane is reduced more by the increased pumping speed than it is increased by the larger gas flow rate. Thus, the more pumps used, the smaller the charge-exchange loss should be. Figure 6 shows the dependence of  $E_p$  on midplane pressure (i. e., number of pumps). It is believed that, as the pumping (and thus the gas flow rate) is increased, a higher and higher percentage of the plasma production is occurring near the electrodes. But in this facility there is still room for improved performance if more pumping speed were available.



## OFF-AXIS AND MULTIPLE SOURCES

Another approach (other than larger diameter cathodes) to making a larger plasma diameter is to move the plasma source radially from the magnetic axis of the mirror machine. The plasma would still be produced by the Phillips ion gage (PIG) electron motion between the opposing cathodes. However, hot particles trapped on off-axis field lines will experience an azimuthal precessional force when they pass through regions of large magnetic curvature. The precessional velocity is given by  $V_p = 2E_{11}/eBR$ , where  $E_{11}$  is the energy related to the component of velocity parallel to the magnetic field line and  $R$  is the radius of curvature of the field line. Thus, in principle, it is possible to form and heat a plasma by an off-axis source and then have the plasma ions precess azimuthally to fill up a larger plasma volume. Whether or not the plasma fills the desired volume depends on whether particles are lost out of the mirror ends or diffuse radially before they have a chance to precess a significant distance azimuthally. The precessional velocity  $V_n$  is proportional to  $E_{11}$ . Thus a charge-exchange collision, which replaces a hot ion with a cold ion, is also detrimental to the precessional process.

A single cathode-anode assembly (with  $a = 7.6$  cm,  $b = 1.3$  cm, and  $c = 1.1$  cm) was arranged such that its centerline was 5.5 centimeters radially removed from the centerline of the magnetic field (fig. 7(a)). Another cathode-anode assembly source of the same dimensions was placed on-axis at the opposite end of the system. With the same gas feed rate as that for an on-axis source, only a faint glow discharge existed, but an annular plasma did fill the desired volume. The cathodes, however, did not become emissive, and the current drawn was less than 50 milliamperes, leading us to believe that the density was too low (probably less than  $10^{11}/\text{cm}^3$ ). The gas feed rate was then increased until the background pressure was greater than  $4 \times 10^{-2}$  newton per square meter ( $3 \times 10^{-4}$  torr). The current was then 100 to 150 milliamperes, and two distinct plasmas could be seen. One was the annular plasma with a mean radius of 5 centimeters, and the other was on-axis with a diameter of approximately 2 centimeters. To the eye the hollow or annular plasma was still quite uniform in the azimuthal direction but the cathode tips, while glowing red, were still not emissive. As the pressure was raised even further, the center discharge suddenly became quite intense, and its behavior was like that in the high current mode discussed in reference 1. Also at this time the on-axis bends in the stainless-steel off-axis cathode holders became emissive and melted soon afterward. Thus, at this high pressure, we had effectively an on-axis plasma source with the exposed cathode holder bends acting as a cathode opposite the center cathode, between which "pigging" action could occur. The off-axis cathode had no opposing cathode for "pigging" and thus its tip never became emissive.

The next step (see fig. 7(b)) was to move the on-axis electrodes to an off-axis position on the same magnetic field line as the original off-axis electrodes. This would make

the "pigging" action more effective. At the same time pieces of tantalum were attached electrically to the floating plates and bent in such a way as to protect the bends in the cathode holders. With this arrangement, the low current mode was achieved with the pressure at  $2.1 \times 10^{-2}$  newton per square meter ( $1.6 \times 10^{-4}$  torr). Because of the higher pressure  $E_p$  was slightly lower than for the on-axis source. To avoid confusion, we henceforth define a source as two opposing cathode-anode combinations situated on the same magnetic field lines.

Next, the off-axis electrodes were each moved 5 centimeters closer to the midplane and tilted slightly so that the centerline of the hollow cathode was more nearly in line with the slightly curved magnetic field direction (see fig. 7(c)). With this scheme, the pressure required to achieve the low current ion-heating mode was lowered to approximately the same as for the on-axis source. Consequently, the value of  $E_p$  was increased. Thus, the off-axis source behaves very similar to the on-axis source when conditions are such that they run in the low-current mode at approximately the same pressure. However, visual observations and NPA scans of the plasma both indicated the hot plasma did not precess any significant distance.

Figure 7(d) shows an arrangement with both a tilted off-axis source and an on-axis source. To start with, the flow rate and applied voltage was the same for both sources. Under these conditions only one of the sources would light (cathodes become emissive) at a given time. Electrically the two sources were in parallel and an unstable situation existed. As one source started to light up, its resistivity decreased, causing more current to flow through that source at the expense of the other one. When the plasma was first turned on after a long shutdown, either source might be the one that would dominate, usually running in the high current cold-ion mode. As that particular source became conditioned and approached running in the low current mode, its resistivity would increase. The other source would then light up and be the dominant source until it too became conditioned. After this process of conditioning each of the sources was nearly complete, it became possible (usually for just a few seconds) to get both sources running simultaneously in the low-current ion heating mode. However, this was the exception rather than the rule. The more likely state was that the sources would flip-flop with one being dominant for a few seconds, and then the other would take over and the first would go out. There were periods when this flip-flopping would continue for more than a minute before one source finally took over for good.

Because of this behavior, it was thought that the on-axis and off-axis sources could be operated simultaneously from the same power supply if separate gas feeds were available. Thus, the gas feed to the on-axis cathode was blocked at one mirror and the feed to the off-axis cathode was blocked at the opposite mirror. The microvalves in the cathode gas feed lines at each end of the system could then be adjusted to control the flow to each source separately. This meant, however, that only one hollow cathode in each

source pair had a high-pressure region inside. The results of the experiments using this arrangement were about what had been hoped for. It was not much easier to get the sources running simultaneously in the low-current mode. But the two sources formed two plasmas that were fairly well spatially resolved.

The results of these experiments have led us to the following conclusions: (1) off-axis sources work as well as on-axis sources when the hollow cathodes' axes are aligned with the local magnetic field lines; (2) it is possible to operate multiple sources from a single power supply if separate gas feed control is provided for each source; and (3) precession of plasma produced by a single off-axis source to fill a larger volume is not possible in the present facility, probably because of high charge exchange-energy losses.

### MASS ANALYSIS OF NPA CURRENT SPECTRA

Most  $I(E)$  of the NPA data presented in this report were taken using only the electrostatic energy analyzer section of the neutral particle analyzer (fig. 8). Complete sweeps of  $I(E)$  against  $E$  can be made in just a few seconds for all masses combined, but the analysis of the spectra according to mass necessitates slow, point by point data taking. The momentum analyzer section of the NPA was used only to obtain typical  $I(E)$  against  $E$  spectra for the three major mass components,  $H^+$ ,  $H_2^+$ , and  $C^+$ . Figure 9 shows  $I(E)$  against  $E$  for typical experimental runs in hydrogen for carbon and tungsten cathodes (carbon anodes). As figure 9 shows, the higher mass species always has the higher average energies. This is consistent with the fact that higher mass particles in crossed electric and magnetic fields should have greater drift energies  $\left[ E_{\text{drift}} = 1/2 m v_D^2 = 1/2 m (E/B)^2 \right]$ . Notice the large mass 12 (carbon) component in figure 9(b) even though tungsten cathodes were used. As more and more runs were taken using these cathodes the magnitude of the carbon component slowly decreased. It is also interesting to note that for tungsten cathodes the  $H^+$  current is a higher fraction of the total current than for carbon cathodes. However, at the time of this report, we do not know the significance to this observation.

### SUMMARY OF BEST RESULTS

One is always interested in the limits of an ion heating scheme. The following shows the best on-axis source results achieved to date in the HIP-1 facility.

Gas	Applied voltage, $V_a$ , kV	Applied field, $B_o$ ,	Pressure, $N/m^2$	$E_p$ , keV
Hydrogen	16	1.5	$1.0 \times 10^{-2}$ ( $7.8 \times 10^{-5}$ mm Hg)	2.4
Deuterium	16	1.5	$0.75 \times 10^{-2}$ ( $5.6 \times 10^{-5}$ mm Hg)	3.7
Helium	14	1.5	$2.8 \times 10^{-2}$ ( $2.1 \times 10^{-4}$ mm Hg)	8

For these cases  $a = 7.6$  centimeters,  $b = 1.3$  centimeters, and  $c = 0.75$  centimeters. The cathodes were tungsten, and the anodes were stainless steel with a tantalum face toward the midplane of the plasma. (See fig. 10.)

For comparison, the best  $E_p$  values obtained in earlier studies with carbon cathodes and anodes were 1.4 keV for hydrogen at 12 kilovolts and 2.1 keV for deuterium at 12 kilovolts. For these cases  $B_o = 1.5$  T,  $a = 7.6$  centimeters,  $b = 1.3$  centimeters, and  $c = 1.1$  centimeters. No results had been obtained with helium.

In the best data with helium, the maximum voltage that could be used was 14 kilovolts. At higher voltages, a high current mode dominated the plasma. The high-current mode resulted in overheating of the electrodes and typically in low ion temperatures. Melt marks were commonly found on the front surfaces of anodes after use. The reason for this high current mode is not understood.

The voltage that could be used with hydrogen and deuterium was limited to about 16 kilovolts because of external breakdown. The porcelain insulated fitting (Alite) where the high voltage passed into the vacuum system had been tested, with the magnetic field on, to more than 20 kilovolts with no gas feed. It is felt that the observed breakdown at voltages well below 20 kilovolts is triggered by large radiofrequency fields associated with plasma noise in the vicinity of the high voltage feedthrough.

The only electron density measurement made thus far with HIP-1 used a microwave interferometer whose beam diameter was larger than the plasma diameter. All that could be said was that the mean electron density of the plasma was greater than  $10^{12}$  per cubic centimeter in hydrogen ( $B_o = 1.13$  T and  $V_a = 8$  kV).

### CONCLUDING REMARKS

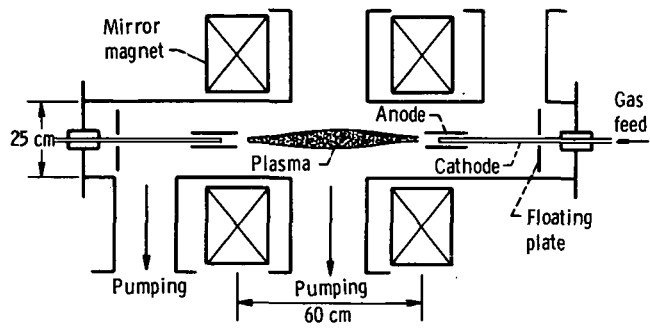
Results of further studies on the Lewis Research Center hot-ion-plasma source (HIP-1) have shown that changes in both the electrode geometry and materials could be made to optimize performance of the facility from the standpoint of producing high ion

temperatures. Ion temperature increased significantly with increased vacuum pumping speed. Sources comprising electrode pairs displaced from the magnetic axis by 5.5 centimeters have been operated and produced high ion temperatures. Both on-axis and off-axis sources can be run simultaneously from a single power supply if their respective gas feed rates are independent. Background pressures in HIP-1, however, are too high to permit significant azimuthal precession of plasma produced by an off-axis source. The analysis of charge-exchange neutrals has been extended to distinguish particles according to mass as well as energy. Under any given plasma condition, the higher mass ions have higher average energies, but not by as much as the ratio of their respective masses.

Lewis Research Center,  
National Aeronautics and Space Administration,  
Cleveland, Ohio, January 2, 1974,  
502-10.

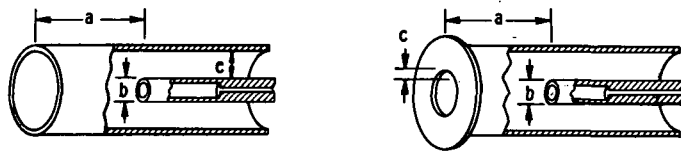
#### REFERENCES

1. Sigman, Donald R.: and Reinmann, John J.: Steady-State Hot-ion Plasma Produced by Crossed Electric and Magnetic Fields. NASA TM X-2783, 1973.
2. Hirose, A.: and Alexeff, I.: Electrostatic Instabilities Driven by Currents Perpendicular to an External Magnetic Field. Nucl. Fusion, vol. 12, no. 3, May 1972, pp. 315-323.
3. Anon.: Thermonuclear Division Annular Progress Report for Period Ending December 31, 1970. ORNL-4688, Oak Ridge National Lab., Aug. 1971, pp. 77-89.



(a) Hot-ion-plasma (HIP-1) source.

HIP-1 electrodes



(b) HIP-1 electrode.

Figure 1. - Experimental apparatus.

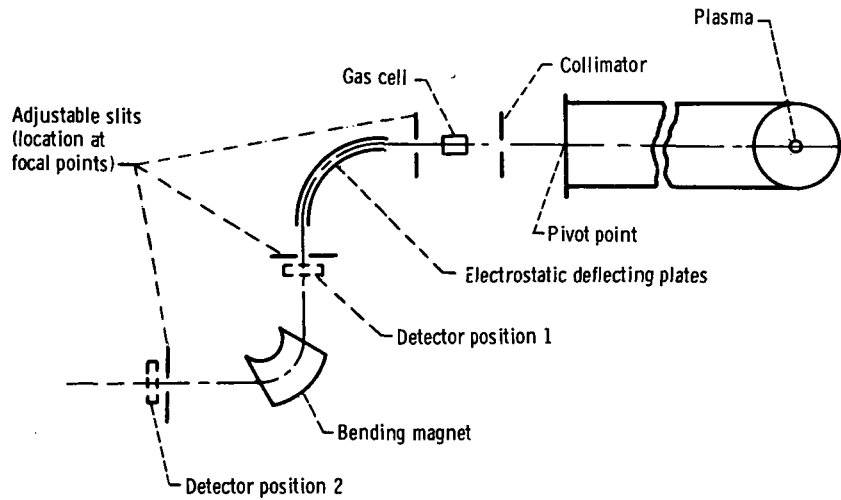


Figure 2. - Change-exchange neutral particle analyzer.

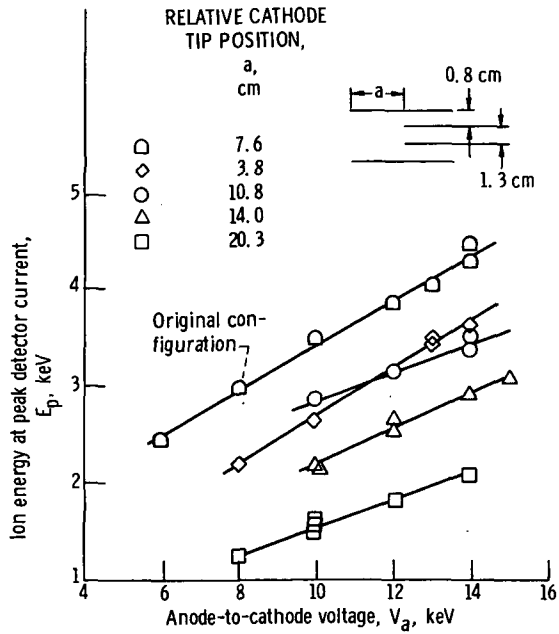


Figure 3. - Ion energy at peak detector current as function of anode to cathode voltage. Gas, helium; midplane magnetic field strength, 1.5 tesla.

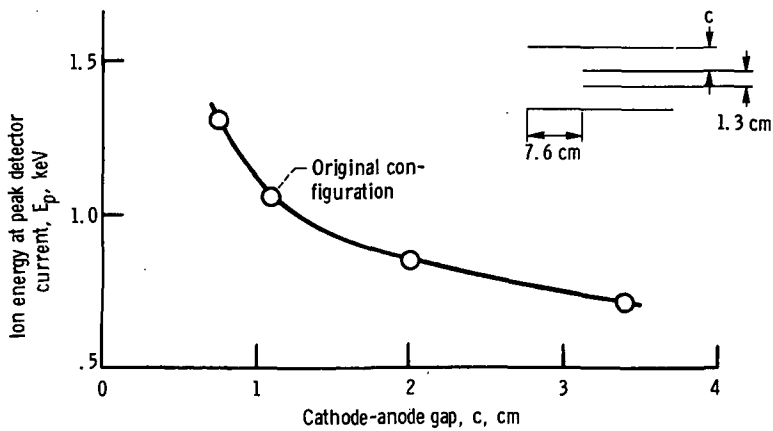


Figure 4. - Ion energy at peak detector current as function of cathode-anode gap. Gas, hydrogen; anode to cathode voltage, 10 kilovolts; midplane magnetic field strength, 1.13 tesla; relative cathode tip position, 7.6 centimeter.

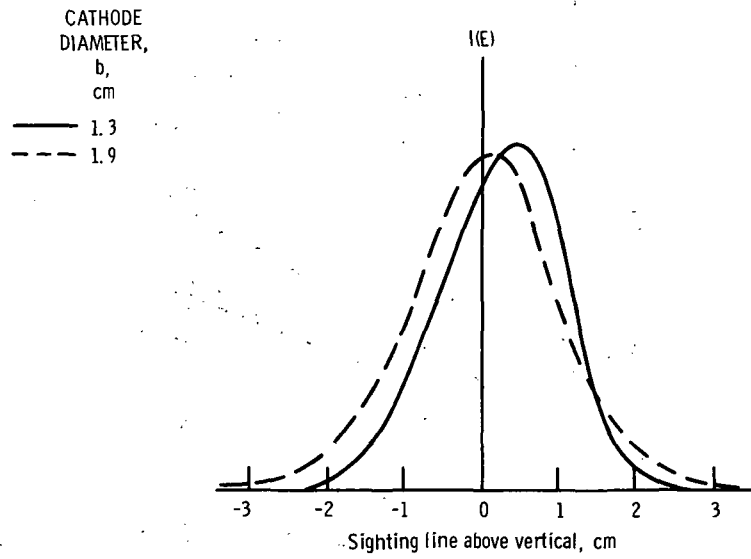


Figure 5. - Neutral particle analyzer traverses for 1.2-keV ions. Gas, hydrogen; anode-to-cathode voltage, 10 kilovolts; relative cathode tip position, 7.6 centimeters; anode-cathode gap, 1.1 centimeters; midplane magnetic field strength, 1.13 tesla.

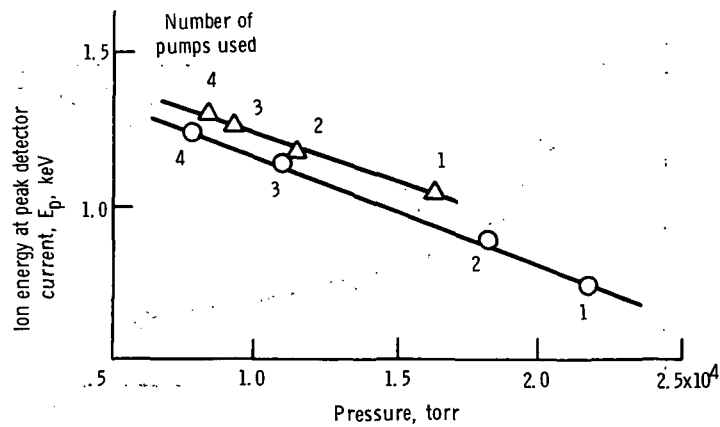


Figure 6. - Ion energy at peak detector current as function of test section pressure. Gas, deuterium; anode-to-cathode voltage, 10 kilovolts; relative cathode tip position, 7.6 centimeter; cathode diameter, 1.3 centimeters; anode-cathode gap, 1.1 centimeters; midplane magnetic field strength, 1.13 tesla.



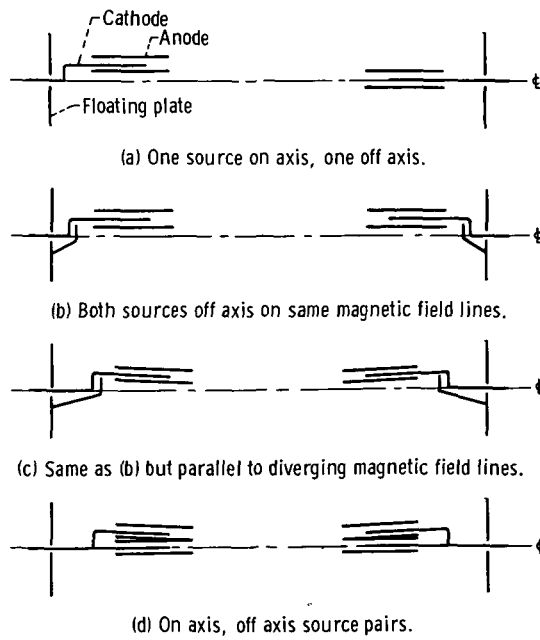


Figure 7. - Various electrode configurations for off-axis experiments.

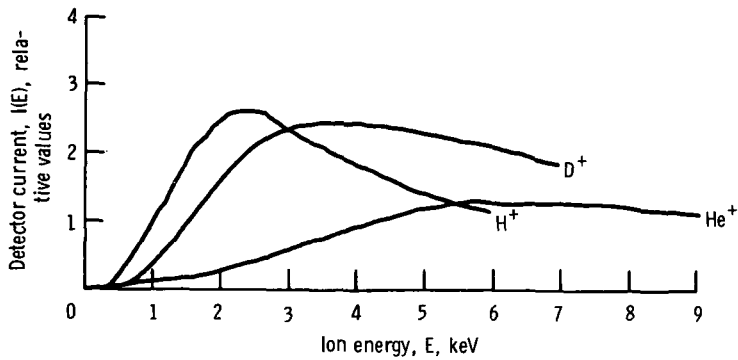


Figure 8. - Detector current as function of ion energy of all plasma components. Midplane magnetic field strength, 1.5 tesla; relative cathode tip position, 7.6 centimeters; cathode diameter, 1.3 centimeters; anode-cathode gap, 0.75 centimeter, anode-to-cathode voltage: for hydrogen and deuterium, 16 kilovolts; for helium, 12 kilovolts.

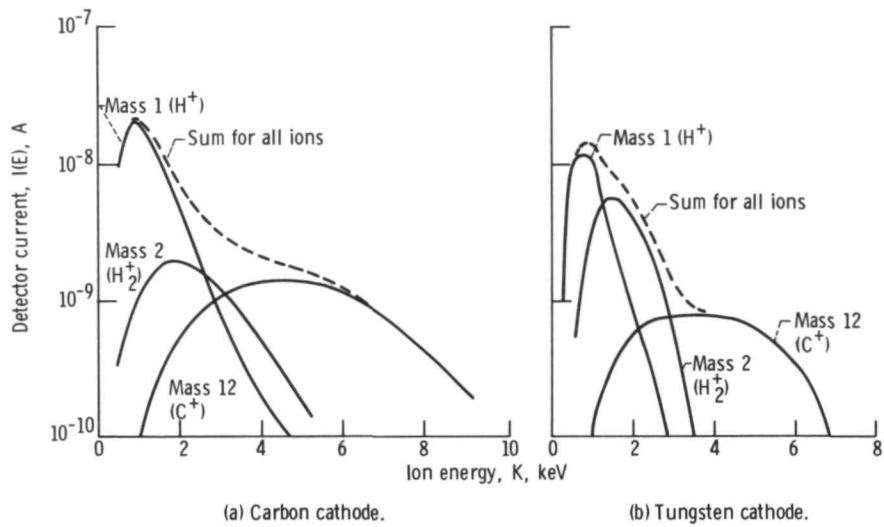
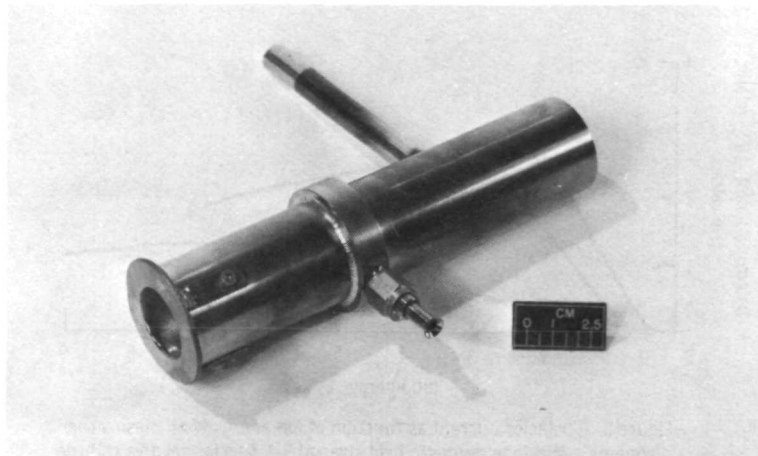


Figure 9. - Detector current as function of ion energy of major plasma components. Gas, hydrogen; anode material, carbon; anode-to-cathode voltage, 9 kilovolts; midplane magnetic field strength, 1.13 tesla.



C-73-3450

Figure 10. - Stainless steel anode with tantalum front face.



POSTMASTER : If Undeliverable (Section 158  
Postal Manual) Do Not Return

*"The aeronautical and space activities of the United States shall be conducted so as to contribute . . . to the expansion of human knowledge of phenomena in the atmosphere and space. The Administration shall provide for the widest practicable and appropriate dissemination of information concerning its activities and the results thereof."*

—NATIONAL AERONAUTICS AND SPACE ACT OF 1958

## NASA SCIENTIFIC AND TECHNICAL PUBLICATIONS

**TECHNICAL REPORTS:** Scientific and technical information considered important, complete, and a lasting contribution to existing knowledge.

**TECHNICAL NOTES:** Information less broad in scope but nevertheless of importance as a contribution to existing knowledge.

**TECHNICAL MEMORANDUMS:** Information receiving limited distribution because of preliminary data, security classification, or other reasons. Also includes conference proceedings with either limited or unlimited distribution.

**CONTRACTOR REPORTS:** Scientific and technical information generated under a NASA contract or grant and considered an important contribution to existing knowledge.

**TECHNICAL TRANSLATIONS:** Information published in a foreign language considered to merit NASA distribution in English.

**SPECIAL PUBLICATIONS:** Information derived from or of value to NASA activities. Publications include final reports of major projects, monographs, data compilations, handbooks, sourcebooks, and special bibliographies.

**TECHNOLOGY UTILIZATION PUBLICATIONS:** Information on technology used by NASA that may be of particular interest in commercial and other non-aerospace applications. Publications include Tech Briefs, Technology Utilization Reports and Technology Surveys.

*Details on the availability of these publications may be obtained from:*

**SCIENTIFIC AND TECHNICAL INFORMATION OFFICE**

**NATIONAL AERONAUTICS AND SPACE ADMINISTRATION**  
Washington, D.C. 20546